Dynamics of Colloidal Glasses and Gels

Yogesh M. Joshi

Department of Chemical Engineering, Indian Institute of Technology Kanpur, Kanpur 208016, India; email: joshi@iitk.ac.in

Annu. Rev. Chem. Biomol. Eng. 2014. 5:181–202

First published online as a Review in Advance on March 19, 2014

The *Annual Review of Chemical and Biomolecular Engineering* is online at chembioeng.annualreviews.org

This article's doi:
10.1146/annurev-chembioeng-060713-040230

Keywords

rheology, soft glassy materials, yield stress, aging, thixotropy, jamming

Abstract

Many household and industrially important soft colloidal materials, such as pastes, concentrated suspensions and emulsions, foams, slurries, inks, and paints, are very viscous and do not flow over practical timescales until sufficient stress is applied. This behavior originates from restricted mobility of the constituents arrested in disordered structures of varying length scales, termed colloidal glasses and gels. Usually these materials are thermodynamically out of equilibrium, which induces a time-dependent evolution of the structure and the properties. This review presents an overview of the rheological behavior of this class of materials. We discuss the experimental observations and theoretical developments regarding the microstructure of these materials, emphasizing the complex coupling between the deformation field and nonequilibrium structures in colloidal glasses and gels, which leads to a rich array of rheological behaviors with profound implications for various industrial processes and products.

INTRODUCTION

The colloids are a varied range of multiphase substances and are ubiquitous in nature and industry (1). Typically colloids are distinguished by the nature of their continuous phase and dispersed phase. The length scale associated with the dispersed phase ranges between 10 nm and 10 μm (2). Of the different variants of colloids, the most common are the ones with liquid as a continuous phase, and depending on the nature of dispersed phase, in which solid, liquid, or gas leads to suspension (or dispersion), emulsion, or foam, respectively. Usually in the limit of small dispersed phase concentration, colloids (with continuous liquid phase) are in the liquid state. With progressive increases in the dispersed phase concentration, the viscosity increases. Beyond a critical concentration, depending on the characteristics of the dispersed phase, viscosity becomes so high that it gives the materials a soft-solid-like consistency such that they do not flow over practical timescales (3, 4). In addition, the microscopic structures of such materials are disordered and may evolve as a function of time. Broadly, such soft-solid-like phases of colloids fall under the category of colloidal glasses and gels, inclusively termed as soft glassy materials (SGMs) (5). Common examples of such materials are concentrated suspensions and emulsions, percolated gels, foams, paints, cosmetic and pharmaceutical creams, mayonnaise, clay debris, cement paste, and a variety of industrial pastes. The rheological behavior of such materials is highly challenging, and poor understanding restricts their analyzability as well as industrial productivity.

The term glass is popularly used for molecular glasses, wherein rapid cooling of a molten glass–forming material causes apparent solidification while preserving the structural disorder (6). Consequently, the material is arrested in a high–free energy state and falls out of thermodynamic equilibrium. Similarly, a rapid increase in the concentration of constituents causes structural arrest in colloidal systems while preserving the disorder associated with the liquid state (2). The resultant soft-solid-like substance is typically represented as a colloidal glass through comparison with the molecular glasses. Therefore, it is not surprising that colloidal and molecular glasses share many similarities (7, 8, 9). Moreover, owing to their easily explorable length scales, the former are studied to understand the microscopic behavior of the latter (2). Colloidal gels, however, are percolated, network-like structures of a dispersed phase within a continuous phase and are governed primarily by attractive interactions. Similar to molecular glasses, colloidal glasses and gels may undergo structural evolution over a period of time. Owing to the close interactions that the constituents share with their neighbors, this class of substances is apparently in the solid state. Upon application of a strong deformation field, however, they flow. This demonstrates the presence of a yield stress, the point at which the solid-to-liquid (or unjamming) transition occurs, which is a prominent characteristic feature of SGMs (10–12). In addition, time-dependent structural evolution and breakdown owing to the imposed stress field induce thixotropy and a variety of other intriguing phenomena, some generic to most substances and some specific to a particular microstructure (3). Owing to the wide-ranging commercial applications and rich physical behavior associated with these substances, this subject has attracted attention from the engineering, chemistry, and physics communities and has grown into an important interdisciplinary research field.

Understanding the rheological behavior of SGMs is extremely important from the industrial point of view. Knowledge of the rheological properties, such as viscosity, modulus, yield stress, and relaxation time, and their dependences on history, deformation rate, and time are vital to design processing equipment, such as reactors, extruders, and mixing vessels. In addition to effective processability, rheological properties of the materials at the end user location are also important. For example, toothpaste or pharmaceutical cream should possess the right value of yield stress so that it does not flow by its own weight over a range of ambient temperatures when not in use, but it should not require excessive stress to make it flow when required. Similarly, it is important that on

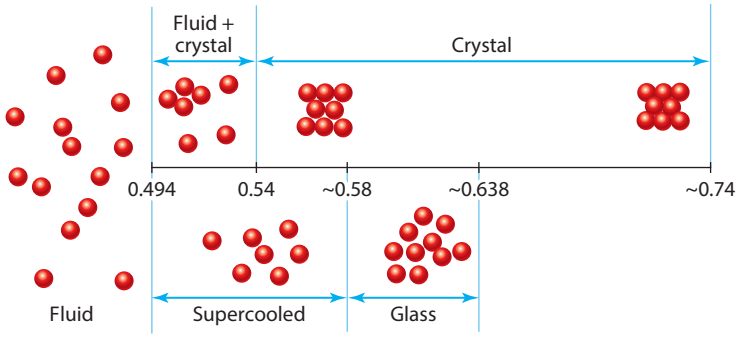

Figure 1

Phase diagram for suspension of monodispersed hard-sphere particles.

a vertical wall, paint should flow easily only under application of a brush or roller but not otherwise. Furthermore, many industrial SGMs become stiff as a function of time owing to aging. Excessive enhancement in stiffness over a period of time might make the materials unusable. Therefore, it is important that the time dependence of structure and rheological behavior is known a priori to design a better product.

Here, we review advances in the field of rheology of colloidal glasses and gels (or SGMs). The purpose of this review is to give a broad picture of the materials, their rheological behavior, and the contemporary issues involved in this topic. Several excellent, detailed reviews on most of these subtopics are available in the literature, which we note below. Dynamic behavior of this class of materials is closely associated with their structure. In the next section, we discuss the nature of the glass phase vis-à-vis the gel phase, as well as different kinds of materials that fall into this category. Next, we discuss the origin and implications associated with the process of physical aging in SGMs. We then focus on the various kinds of rheological behaviors shown by SGMs, and we present theoretical developments on this topic to capture the experimental observations. Finally, we present some concluding remarks.

STRUCTURE OF COLLOIDAL GLASSES AND GELS

Particulate Glasses

Interparticle repulsion is primarily responsible for a particulate glassy phase. We first consider a very simple case of suspension of monodispersed spherical particles involving only hard-sphere interactions, wherein the potential is zero if the particles are not touching and otherwise infinite (11). This prevents the particles from interpenetrating. Consequently, all the possible configurations have identical (zero) potential energy, thereby allowing the maximization of entropy to characterize the equilibrium state (13). **Figure 1** presents the phase diagram of such a suspension of monodispersed hard spheres (2, 13, 14). Clearly, at low volume fractions (ϕ_v), the suspension is in a fluid state. Upon increasing ϕ_v slowly beyond 0.494, crystals with $\phi_v = 0.545$ start nucleating and coexist with the fluid phase. Beyond $\phi_v = 0.545$, only the crystalline state exists. With further increases in ϕ_v, the crystals become compact up to $\phi_v \approx 0.74$, which is the maximum packing fraction associated with the face-centered cubic or hexagonal close packing (13).

If ϕ_v is increased quickly from the fluid state, thereby preventing nucleation of crystals, the suspension enters the so-called supercooled regime (2). In this regime, individual particles can be considered to be arrested in cages formed by their neighbors. Owing to thermal motion, the particle

rattles inside the cage before escaping (diffusing). This cage-diffusion timescale, also known as α relaxation time (τ_α), increases with ϕ_v and diverges as $\phi_v \rightarrow 0.58$, the concentration associated with the colloidal glass transition (15). Monodispersed spherical particles can exist in the random disordered configuration up to only $\phi_v = \phi_{rcp} \approx 0.64$, the random close-packing fraction. ϕ_{rcp} increases with polydispersity. The elasticity of particulate glasses originates in caging, as discussed below.

In practice, closer match to hard-sphere interaction is obtained by inducing short-ranged repulsion among the particles, either by absorbing a small layer of a polymer or via electrostatic interactions (16). Experimentally, the suspension of monodispersed particles has a strong tendency to crystallize. Therefore, to observe the supercooled region and glass transition, polydispersity greater than 8% is maintained (2). Recently, multi-arm star polymer and hairy nanoparticle melts have been widely studied in literature. These materials qualitatively behave similar to suspensions of hard-sphere particles, with additional relaxation modes originating from the arm entanglements (17, 18). Similar to the case of isotropic particles, anisotropic particles also undergo a glass transition corresponding to ϕ_v that decreases with increases or decreases in aspect ratio (r) (11). Particularly for rodlike particles ($r > 1$), the glassy domain is observed to exist in the range of $0.7 < r\phi_v < 5.4$ (19).

Electrostatic interactions: interactions originating from interacting charged surfaces

van der Waals interactions: interactions resulting from fluctuating dipoles of atoms and molecules of two interacting surfaces

Depletion attraction: attraction induced between particles owing to the presence of nonabsorbing polymers in solvent, which causes a depletion zone near the particle with different osmotic pressure than the bulk

Fractal dimension (d_f): for a three-dimensional object, fractal dimension is a power law exponent that relates the mass (M) to the length scale (R), given by $M \propto R^{d_f}$

Particulate Gels

Particulate gels are formed owing to short-range but strong attractive interactions among the particles. The most prominent attractive interactions that colloidal particles share are van der Waals interactions, electrostatic interactions, and depletion attraction (13, 14). The presence of attractive interactions leads to the formation of fractal aggregates with a radius of gyration (R_a), so that the volume fraction of particles in a cluster is given by $\phi_i = (R_a/R_p)^{d_f-3}$, where R_p is the particle radius and $d_f (1 < d_f < 3)$ is the fractal dimension. The volume fraction of aggregates is given by $\phi_a = \phi_v/\phi_i$ (20). Colloidal gelation occurs when aggregates become sufficiently large to touch each other, which typically can be considered to occur at $\phi_a = \phi_{rcp}$ (3). Elasticity of a particulate gel is due mainly to the elasticity of the backbone network in aggregates and not to the interaggregate links (3).

In principle, the gel formation is possible at very low ϕ_v if attractive interactions are very strong (21). Typically, if collisions among the particles lead to strong bond formation, the resulting aggregate is more open, with small d_f ranging from 1.7 to 1.9. Instead, if multiple collisions are required owing to a repulsive barrier, the aggregate is more compact, with d_f ranging from 2 to 2.1 (11, 22).

In the literature, the term attractive glass is also used to represent a phase dominated by attractive interactions but with high ϕ_v comparable to that of glasses (23, 24). With a decrease in ϕ_v, a gel phase is obtained. However, with a decrease in attractive potential (U/k_BT), a gel phase changes to an equilibrium liquid, and an attractive glass changes to a repulsive glass. The complete phase diagram with respect to U/k_BT and ϕ_v for bi-disperse sticky particles is discussed in Reference 23. Interestingly fluidization upon decreasing ϕ_v as well as U/k_BT is also proposed by a jamming phase diagram for colloidal gels (25, 26). This diagram is shown in **Figure 2**, which also describes unjamming upon application of stress in addition to the effect of U/k_BT and ϕ_v.

Finally, in a particulate suspension, the colloidal glassy and gel state can be distinguished based on the length scale beyond which the density becomes homogeneous. In particulate colloidal glasses, this length scale is close to the interparticle distance, whereas in gels it is approximately the aggregate length scale (24).

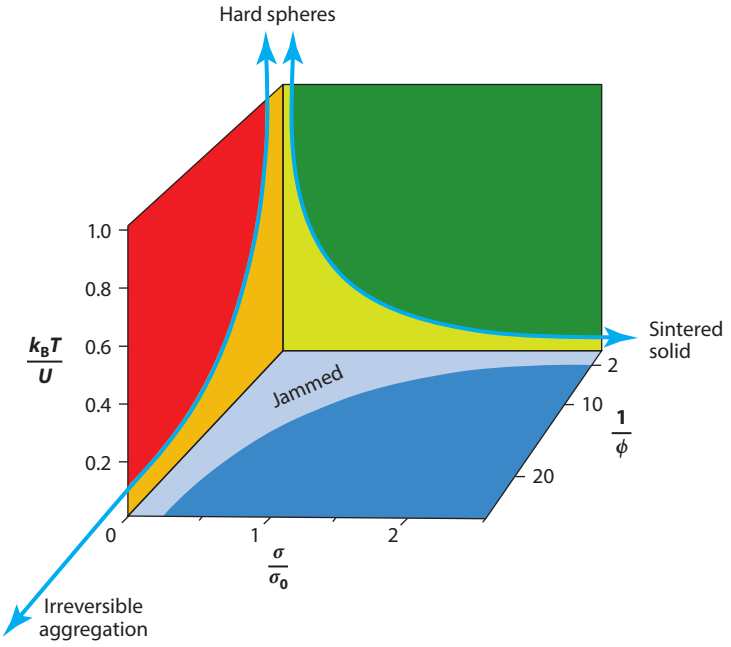

Figure 2

Jamming phase diagram for attractive colloidal particles. The diagram suggests that decreasing interparticle interactions (or increasing temperature), increasing stress, and decreasing concentration causes unjamming transition. Reprinted from Reference 26 with permission from Macmillan Publishers Ltd. *Nature* ©2001.

Concentrated Emulsions, Microgel Pastes, and Foams

In concentrated emulsions, microgel pastes, and foams, the continuous phase is liquid, whereas the dispersed phase is liquid, soft deformable solid, and gas, respectively. Interestingly, these materials share many structural and behavioral similarities owing to repulsive interactions shared by the dispersed units (27, 28). In emulsions and foams, the dispersed phase is in the form of droplets or bubbles that are stabilized by surfactants/particles, whereas in microgel pastes the dispersed phase consists of swollen polymeric submicrometer-sized gel particles. It is generally observed that at low ϕ_v, these materials are in a fluid state. At concentrations above ϕ_{rcp}, the drops/bubbles/particles of the dispersed phase get deformed owing to steric constraints and demonstrate finite elastic modulus and yield stress (27–29), features reminiscent of a soft glassy state. Owing to the deformable nature of the dispersed phase, volume fractions approaching unity can also be obtained. At very high concentrations, the dispersed units assume polygonal shapes with flat interfaces. Elasticity of the emulsions and foams originates from surface tension, whereas that of microgel pastes arises from the osmotic pressure of intersegmental interactions of the associating polymer network.

Other Model and Industrial Soft Glassy Materials

Several other systems that have been studied in the literature show structural disorder and glassy dynamics. One prominent system is a suspension of platelike clay particles, such as Laponite and Bentonite ($r^{-1} = 10$ to 1,000). Usually, addition of more than one volume% of clay in water converts the free-flowing liquid to the soft solid with finite modulus (30). The microstructure responsible for this is believed to result from the repulsive as well as attractive interactions (31–33).

Highly filled polymer melts and polymer-clay nanocomposites also demonstrate jamming above a critical concentration (34, 35).

Many products and intermediate raw materials associated with the chemical and allied industries have soft-solid-like or pasty composition. For example, the mining industry encounters drilling muds (36) and slurries. The home- and personal-care-product industry deals with cosmetic pastes (37), toothpastes, foams (28), and dishwasher and laundry detergent pastes (38). Other examples include paints (39), pastes used in pharmaceutical and agrochemical industries (40), ceramic and cement pastes (41), greases, waste water (42), and a variety of pasty food products (37). Although the microstructures of most of the commercial materials are rather complex and not well defined, their physical behavior is reminiscent of various features discussed in this paper. Owing to the presence of a yield stress and thixotropy, effective processing of these materials to form useful products has been and continues to be a challenge.

Age: for soft glassy materials, age is defined as time elapsed since shear melting (or rejuvenation)

Autocorrelation function ($g_2 - 1$): measure of how fluctuations in intensity separated by time t are correlated (for complete correlation = 1, for no correlation = 0); its decay is therefore a measure of relaxation dynamics

PHYSICAL AGING

Colloidal glasses and gels are usually thermodynamically out of equilibrium owing to the restricted mobility of their constituents, which allows only limited access to their phase space (25). Owing to their natural instinct to achieve equilibrium, in a process of physical aging, their structure evolves to lower the free energy, and the rate of aging gradually slows down with time (43). However, physical aging is possible only if the constituents have sufficient mobility, which is usually the case with colloidal materials. Technically, a system can be taken out of equilibrium in a trivial sense simply by perturbing the equilibrium materials. However, the consequent transient to reestablish the equilibrium state differs from that of physical aging, wherein the timescale over which a material relaxes increases with time (5).

During aging, in the absence of any other imposed timescales, the natural timescale available to a material is its age (t_w), which imposes $\tau \propto t_w$ (44). This linear regime, known as the full aging regime, is described in **Figure 3*a***, wherein the autocorrelation function ($g_2 - 1$) is plotted against time for polystyrene suspensions with different t_w. The autocorrelation function shows a two-step decay, with the short and the long time decays representing τ_β (β timescale) and τ_α, respectively. It can be seen that τ_α scales linearly with t_w (7, 45). Rather than showing linear dependence, however,

Figure 3

(*a*) Decay of autocorrelation function at different t_w for 50% polystyrene suspension. The decay representing α mode slows with an increase in t_w. The inset shows that τ_α scales linearly with t_w. Reprinted with permission from Reference 35 ©2003 R. Soc. Chem. (*b*) Evolution of G' for 3% Bentonite suspension at different temperatures (T) from 5°C to 80°C. Evolution shifts to low t_w with an increase in temperature. The inset shows superposition of G'. Reprinted with permission from Reference 60 ©2007 Am. Phys. Soc. (*c*) Frequency dependence of G' and G'' at different concentrations of silica suspension. With an increase in concentration, suspension undergoes a liquid-to-glass transition. The line passing through the data is a fit of mode-coupling theory. Data from Mason & Weitz (77). (*d*) Frequency dependence of G' and G'' as a function of concentration of carbon black in oil. An increase in concentration changes the behavior from liquid-like to solid-like. Reprinted with permission from Reference 22. (*e*) Stress versus strain-rate flow curves for different Carbopol solutions to determine yield stress. The line passing through data is a fit to the Herschel-Bulkley model. In the inset, G' (*squares*) and G'' (*circles*) are plotted as a function of deformation. Reprinted with permission from Reference 86 ©2013 R. Soc. Chem. (*f*) Strain induced in 5% Bentonite suspension under application of different creep stresses. Stress increases from bottom to top. Reprinted with permission from Reference 52 ©2006 Soc. Rheol. (*g*) Evolution of G' and G'' under application of oscillatory stress field of varying magnitude for 2.8 wt% Laponite suspension. An increase in magnitude of stress shifts the evolution to high times. Data from Shukla & Joshi (105). (*h*) Shear banding in thixotropic yield-stress fluid composed of clay-loaded emulsion in a cone-and-plate rheometer for different globally imposed shear rates. Adapted from Paredes et al. (109) with permission of IOP Publ. All rights reserved. (*i*) Effect of concentration on shear-thickening behavior of polyvinyl chloride suspension. Beyond 51% concentration, discontinuous shear thickening is observed. Data from Hoffman (133).

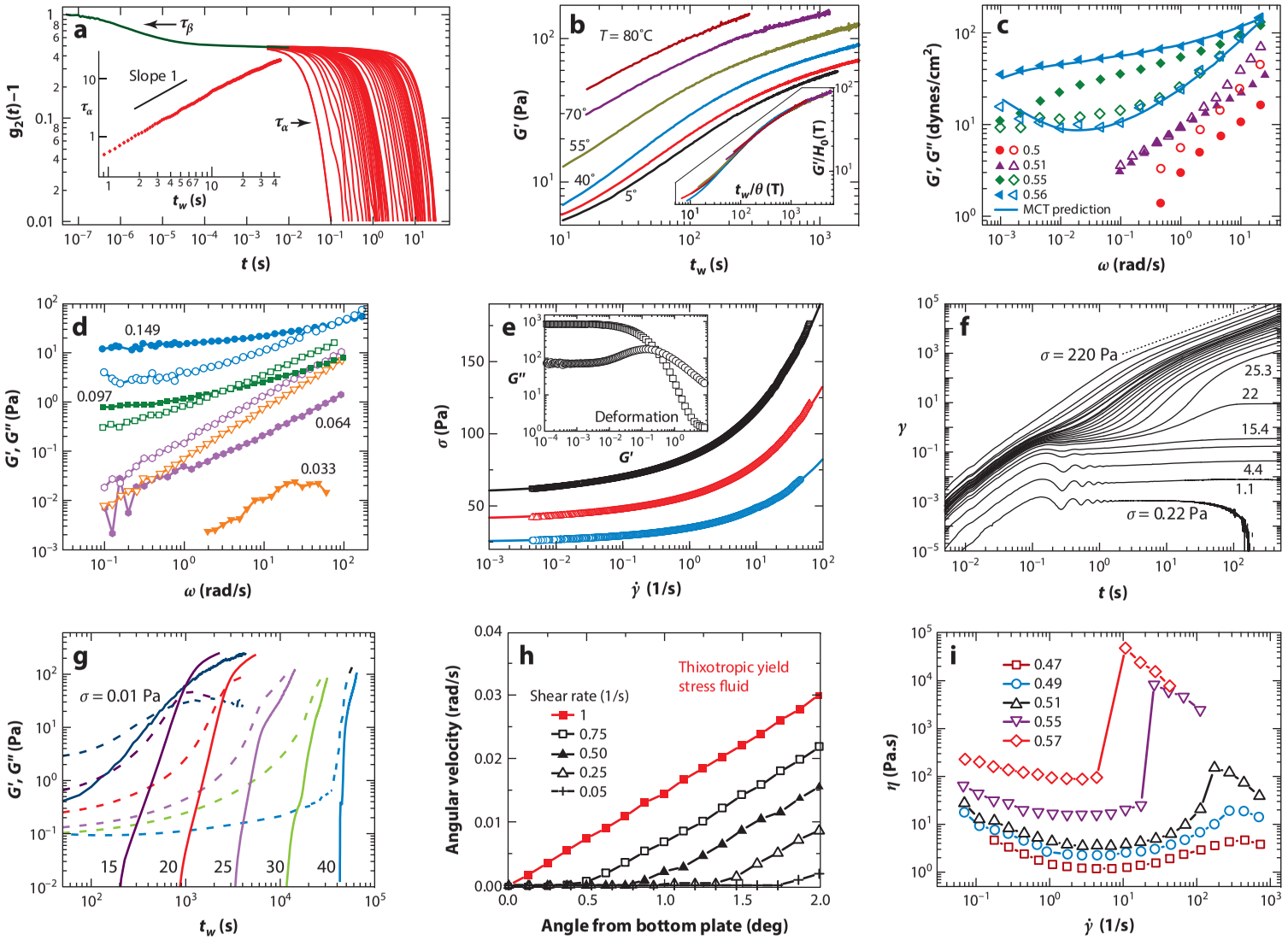

many SGMs usually exhibit power law dependence: $\tau \propto \tau_0^{1-\mu} t_w^{\mu}$, where μ is the power-law exponent and τ_0 is the microscopic time (5–7, 46, 47). In the literature, various SGMs have been reported to show subaging ($\mu < 1$) (48, 49) or hyperaging ($\mu > 1$) behaviors (46, 50, 51). The physical reasons for such behavior, along with its implications, have been discussed in the literature (43, 46).

Microscopically, the entities or particles that constitute SGMs are considered to be present in energy wells (physical or energetic cages) with potential $U(r)$. Unlike liquids, the thermal energy associated with the entities of SGMs is significantly smaller than the average well depth (E), which allows their thermally activated diffusion out of the wells only occasionally (5). The mean cage diffusion or relaxation time is postulated to have an Arrhenius dependence on E given by $\tau = \tau_0 \exp(E/k_B T)$ (5). If a is characteristic length scale, the modulus of SGM is given by $G = (d^2U/d\gamma^2)_0/a^3$, where subscript 0 indicates the minimum of the well ($r = a$) and $\gamma = \langle r - a \rangle / a$ (3, 13). $U(r)$ can be broadly represented by $U(r) = Ef(r/a)$, where $f(1) = -1$ (13). This leads to $G \propto E/a^3$, in which G is expressed as the energy density. Because E increases with t_w during aging, enhancement of τ and G can be considered as rheological manifestations of the aging process. If we combine $\tau = \tau(t_w)$ and $\tau = \tau(E)$, we obtain $G \propto (\mu k_B T/a^3) \ln(t_w/\tau_0)$ (46). Interestingly, G of many SGMs indeed demonstrates logarithmic dependence on time (49, 52–54). By virtue of a distribution of well depths, there also exists a spectrum of relaxation times (5, 44). At the particle level, the depths of the energy wells increase with time. Consequently, in a physical aging process, the whole spectrum of relaxation times evolves to higher values (54). For some SGMs, the change in τ as well as G is extremely sluggish; therefore, for all practical purposes, the aging in such materials can be considered to be absent.

The origin of the aging process is specific to the microstructure of the SGMs. In the case of concentrated suspensions of hard spheres, aging is entropy driven (2). Interestingly, a recent study indeed provided evidence of a free-energy decrease during aging (56), and in multi-arm star glasses, aging has been observed to lead to crystallization (57). In the case of suspensions of attractive particles, the structural evolution involves an alteration of the fractal network or strengthening of the interparticle bonds with t_w (58). In the case of systems like concentrated emulsions or microgel pastes, where thermal forces are not dominant, the drive for structural evolution is through the relaxation of internal stresses that arises from elastic energy stored in the deformed drops/gel particles. Cipelletti & Ramos (43) suggested that when the internal stress relaxation drives structural recovery, the modulus decreases with t_w. However, at least for concentrated emulsions, there are reports suggesting otherwise (39, 59).

Temperature has a profound effect on aging behavior. In **Figure 3*b***, the evolution of elastic modulus (G') of aqueous Bentonite suspension measured at different temperatures (t_w) by Ovarlez & Coussot (60) is plotted as a function of t_w. Evolution shifts to lower t_w as T is increased, while the curvature is preserved. Consequently, the horizontal and vertical shifting lead to a superposition, as shown in the inset. This behavior suggests that the process of aging is faster at higher temperatures, which is attributed to enhanced thermal energy (53). Similar observations of enhancement in the rate of aging upon increase in temperature have been reported for aqueous suspensions of Laponite (53, 61, 62), mustard (60), microgel paste (8), polymer clay nanocomposites (35), and suspensions of hairy nanoparticles (63). Rather than carrying out aging under isothermal conditions, application of step-up or step-down temperature jumps during aging is expected to expedite or slow down the subsequent processes, respectively. However, the path that the system takes subsequent to the step-up or step-down temperature change has been observed to be asymmetric for SGMs owing to nonlinear physical effects associated with the temperature change (8, 62).

Many commercial SGMs also demonstrate physical aging when kept under rest (storage), which enhances their stiffness as a function of time, making them unsuitable for intended applications.

Therefore, the knowledge of the period over which a material of given composition remains useful, also known as shelf life, is extremely vital to the industry. For many products with a paste-like consistency, one of the routinely used test protocols to predict shelf life is called the accelerated heat stability test, wherein the state of a sample after preservation for 14 days at 54°C is considered to be equivalent to its state after two years under ambient conditions (40). However, this test does not yield desirable results owing to different rates of aging arising from different microstructures. Although further discussion on issues associated with the physical behavior of commercial SGMs is beyond the scope of this review, there is huge potential for further work in this field to improve productivity and material behavior.

RHEOLOGICAL BEHAVIOR

The prominent feature of colloidal glasses and gels is their apparent solid-like nature. By decreasing concentration or by reducing attractive interactions, fluidity can be induced in such systems (unjamming). However, for a material with a given composition, application of a deformation field induces unjamming by yielding, as described in **Figure 2** (26). Moreover, the role of the deformation field is not limited to yielding; depending upon the nature of SGMs, the physical properties and the rheological behavior are profoundly influenced.

Rheological behavior is primarily studied using a rotational rheometer, an instrument that measures stress/strain in response to applied controlled strain/stress. For SGMs, the response of rate-controlled experiments often differs from that of the stress-controlled experiments owing to their strong history dependence. Many recent studies have employed superposition of two flow fields, such as rotation and compression/tensile (64, 65) and creep and oscillations (60, 66), to study the response of such mixed flow fields. Typically, a rheometer gives macroscopic information averaged over the thickness of a shear cell in which the local velocity field is unknown. Hence, many additional in situ tools have been employed to assess the velocity field, details of which are reviewed in References 67 and 68. In SGMs, rheology and structure strongly influence each other; therefore, knowledge of the structural changes that occur in a rheometer gives significant insights into the underlying dynamics. Various probes, such as microscopy and laser light/X-ray/neutron scattering, have been used in the literature that render information not only about structure but also about the relaxation dynamics of the SGMs under shear (44, 45, 69–71). Along with rheometers that explore macroscopic length scales, microrheological tools have also been used to investigate SGMs. In microrheology, the motion of micrometer-sized particles embedded in SGMs is probed. The motion may be due to thermal energy (passive microrheology) or to the application of an external force (active microrheology). The details of microrheology are reviewed in References 72 and 73. Owing to the different length scales probed by microrheology, its results differ from those of the conventional rheometers (74). Furthermore, the varying size of the probe particles gives profound information about the length scales associated with the structure being probed (75).

In the limit of linear viscoelasticity, where the deformation field does not influence the structure of the material, application of an oscillatory flow field gives insight into its nature. In **Figure 3*c*** and ***d***, the effect of concentration on frequency dependence of elastic (G′) and viscous (G″) moduli for a model particulate glass (silica suspension having hard-sphere interactions) (76) and a particulate gel (carbon black in oil) (77) is plotted. For small concentrations, $G'' > G'$ indicates a liquid-like behavior. However, at higher concentrations, G' dominates and also demonstrates a plateau in the limit of small frequencies, indicating a solid-like behavior. For colloidal glasses, G'' exhibits minima at high concentrations. Winter (78) provided insight into the rheological response of a glass vis-à-vis a gel by estimating the relaxation time spectrum for these two microstructures, and

Linear viscoelasticity: viscoelastic behavior characterized by linear relationship between stress, strain, and their time derivatives

Elastic (G') and viscous (G'') moduli: measures of energy stored (elastic) and dissipated (viscous) during a strain cycle; for an oscillatory strain input $\gamma = \gamma_0 e^{i\omega t}$ and stress output $\sigma = \sigma_0 e^{i(\omega t+\delta)}$, elastic and viscous moduli are $G' + iG'' = (\sigma_0/\gamma_0)e^{i\delta}$

found them to obey a power law. However, the power-law exponent for particulate glasses was observed to be positive, whereas that for the gels at the gel point was negative. The origin of this difference was attributed to the dominance of fast modes in gels compared with that of slow modes in glasses at the liquid-to-solid transition (78).

Despite their differences, because glasses and gels share many rheological similarities, we treat them generically as SGMs. In addition, SGMs have also been differentiated based on whether thermal fluctuations play any role, and the corresponding liquid-to-solid transition has been termed the glass transition, or jamming transition (79). However, in many studies, the term jamming transition has been used generically to represent liquid-solid transitions in SGMs (12). In this review, we subscribe to this latter view. In SGMs in which aging is present, the deformation field reverses aging by destroying the structures evolved during the aging and inducing mobility among the constituting entities. This process is known as rejuvenation (7). In the case of complete rejuvenation, when all the constituents of SGM undergo cage diffusion, complete obliteration of aging throughout the sample stops the time dependence. For SGMs that show a power-law dependence, $\tau \propto \tau_0^{1-\mu} t_w^{\mu}$, μ usually has a constant value for small σ, which gradually decreases with increased σ and approaches zero in the threshold-stress limit known as yield stress (σ_y) (54, 80, 81). In any rheological experiment, to get a uniform and repeatable initial state, it is mandatory to preshear the material at $\sigma > \sigma_y$. However, changing the stress level beyond σ_y during shear melting affects neither the state of the sample nor the subsequent structural recovery (44, 82). The time-dependent decrease in viscosity under application of flow field, and subsequent recovery when flow is stopped, is known as thixotropy (11), and it is a common feature of many SGMs. Various characteristics of thixotropy have been discussed in detail in recent reviews (11, 83). Members of the class of materials in which σ_y increases with time (84) are termed thixotropic yield-stress materials (85).

The materials that show σ_y but not thixotropy are known as simple yield-stress materials. In such materials, time dependency is absent, and σ_y remains constant (85). In **Figure 3*e***, a typical stress–strain rate behavior of a model yield-stress material (Carbopol gel) is plotted (86), in which σ reaches a constant value as shear rate $\dot{\gamma} \rightarrow 0$. The inset shows yielding under oscillatory flow field with increasing strain, wherein at the onset of yielding (decrease in G'), G'' shows a maximum describing energy dissipation. The intensity of the maximum, however, depends upon the frequency (87). The concept of σ_y is discussed in great detail in the traditional rheology literature. In his famous review, Barnes (88) claimed that the true σ_y does not exist and that material merely undergoes a dramatic transition from very slow to rapid flow. In addition to questioning the very existence of true σ_y, the literature also reports poor reproducibility associated with the measurement of σ_y. In an important contribution, Bonn and coworkers (85) claimed that σ_y is a true property and argued that previous studies did not take proper precautions to ensure a steady state while estimating viscosity.

Interestingly, the presence of a true σ_y raises an important question on the validity of a famous quote, "Πάντα ῥεῖ," or "Everything flows," usually attributed to Heraclitus (88). However, it should be noted that the concept of everything flows is applicable to systems whose equilibrium state is a liquid state with finite relaxation time. If at the equilibrium state the SGM does not relax on any timescale (classical elastic solid state), it shall never flow unless the equilibrium structure is destroyed by applying a finite stress. We believe that such materials should demonstrate true σ_y.

Von Mises proposed that, when the applied deformation field is two- or three-dimensional (velocities and gradients in multiple directions), a material flows when the second invariant of the stress tensor exceeds the σ_y (89). Although von Mises's law is approximately a century old, it was validated only recently for SGMs by Ovarlez et al. (64) and later by Shaukat et al. (65).

Microstructure profoundly affects the yielding behavior of SGMs. Materials with dominant repulsive interactions usually show a single step yielding, whereas those with attractive interactions

(gels) show a two-step yielding (90–93). The yielding in the former is attributed to cage diffusion, whereas two-step yielding in the latter is ascribed to network breakage followed by cluster rupture. Recently, two-step yielding has also been reported for binary hard-sphere colloidal glasses (94) and for dense suspensions of anisotropic particles (95).

Thixotropic yield-stress materials show very rich rheological phenomena. Rheology of such SGMs is dictated by competition between aging and rejuvenating relaxation modes. As discussed before, the spectrum of relaxation times is related to the distribution of energy well depths (barrier heights, E_i) occupied by the particles through the Arrhenius relationship, $\tau_i = \tau_0 \exp(E_i/k_BT)$. Eyring's (96) classical proposal suggests that the stress applied to a material reduces the barrier height linearly: $\tau_i = \tau_0 \exp[(E_i - e_d)/k_BT]$, where e_d is the energy raised by the applied deformation field. Eyring (96) proposed that $e_d = \sigma V^*$, where V^* is activated volume, whereas Sollich et al. (97) proposed that $e_d = k\gamma^2/2$, where γ is strain and k is the spring constant. Both these expressions suggest an alteration of the relaxation-time spectrum under the action of the deformation field, as the particles residing in shallow wells (low E_i) are more vulnerable to undergo cage diffusion. Interestingly, particulate glasses have been observed to sustain up to 15% of strain before flowing, a phenomenon attributed to cage elasticity (98). Thixotropic SGMs demonstrate a very rich variety of rheological behaviors, such as overaging, viscosity bifurcation, delayed yielding, delayed jamming, and shear banding. All these effects originate from competition between aging and rejuvenation and, in some cases, how the deformation field affects the spectrum of relaxation times, and all are discussed below. In addition, we also discuss the shear-thickening behavior associated with hard-sphere suspensions that originates from its jammed state.

Overaging

Overaging is a phenomenon exhibited by various SGMs, wherein the application of moderate magnitudes of deformation causes the relaxation dynamics to slow down rather than to speed up. Viasnoff and coworkers (44) were the first to observe overaging. They applied bursts of oscillatory flow field to a 51% polystyrene suspension with different ages and reported that for moderate bursts the relaxation time increases beyond without any burst. They observed that the shape of the relaxation-time spectrum changes with application of burst, wherein fast modes become faster and slow modes become slower. They argued that during overaging, the deformation field forces diffusion of particles occupying shallow wells, thereby overpopulating the deeper wells while simultaneously populating further shallow modes and modifying the spectrum into a bimodal. Interestingly, overaging has been reported not just for other SGM, such as Laponite suspensions (99), but also for polymer glasses (100). Recently Kaushal & Joshi (101) proposed that the forced cage diffusion of the particles residing in the shallow wells by the application of a deformation field can be used as a tool to control the relaxation time spectrum of SGMs.

Viscosity Bifurcation/Delayed Yielding

Coussot et al. (102) carried out creep tests on several SGMs and observed that there exists a very narrow range of shear stress below which the material undergoes solidification and above which it flows, as shown in **Figure 3*f***. They defined the lowest achievable steady shear rate as the critical shear rate below which aging is believed to dominate. They termed this phenomenon viscosity bifurcation. Sprakel et al. (103) also observed an apparently similar phenomenon wherein they performed creep experiments on different types of gels but reported two distinct exponential regimes of dependence of time to yield on applied stress, suggesting the possibility of delayed yielding no matter how small the stress is. A similar phenomenon was also reported for a Laponite

suspension (54) and a thermo-reversible silica suspension gel (104). Baldewa & Joshi (54) proposed that a fine balance between aging and rejuvenating modes altered by the strain field leads to such behavior.

Delayed Solidification

Contrary to the observations of delayed yielding, Shukla & Joshi (105) observed that a Laponite suspension shows sudden solidification even after being sheared under a stress-controlled oscillatory flow field for a very long time, with initial strain of the order of 1,000% to 20,000%, as shown in **Figure 3*g***. Such behavior cannot be explained by conventional theories, as the assumed affine deformation throughout the material will always lead to complete rejuvenation for realistic energy well depths. Joshi et al. (106) suggested that under a strong flow field, suspension might be composed of solid pockets surrounded by the fluidized suspension. The small strain in the boundary layer of the pockets might cause growth of the solid regions owing to aging. Such a growth is expected to reduce the magnitude of the oscillatory strain, increasing the rate at which the solid regions grow. Finally, through a forward-feedback mechanism, the solid region suddenly occupies the space, causing the delayed solidification of the material.

Shear Banding and Wall Slip

Shear banding represents the observation of discontinuity in shear rate in the flow domain during the steady state. In simple yield-stress fluids, shear banding originates from the variation of stress in the flow field, such that flow occurs in the region where $\sigma \geq \sigma_y$, and the velocity gradient is zero in the region where $\sigma < \sigma_y$ (107, 108). However, in thixotropic yield-stress fluids, shear banding is observed even though the stress variation over the flow domain is negligible. If the imposed shear rate is less than the critical shear rate (the rate below which steady state cannot be achieved owing to the dominance of aging), the flow field is divided into two bands, and only one band flows at the critical shear rate (85, 108). An example of such banding is shown in **Figure 3*b***, in which a clay-loaded emulsion shows shear banding for global shear rates smaller than the critical shear rate (109). Shear banding has also been observed in start-up flows (110). Moorcroft et al. (111) developed a criterion for the observation of shear banding for such transient flows that solely depends on the shape of the rheological response function. Shear banding has been reported for Carbopol gels (112), clay suspensions (113, 114), emulsions and foams (109, 115), graphene oxide dispersion (116), and cement pastes (41) in recent reviews including discussions on the physical behavior (108) and probes (67). Recently, Besseling et al. (117) reported the presence of shear banding in hard-sphere suspension owing to the concentration variations arising from migration of particles toward domains of low shear rate. They argued that even for small concentration variations, the strong dependence of the yield stress on concentration leads to shear banding.

Owing to the arrested structure that spans macroscopic length scales, SGMs tend to slip on the walls of a rheometer. Slip has been reported for variety of SGMs, including particulate glasses (118, 119), colloidal gels (120, 121), emulsions (122, 123), foams (28, 124), commercial and microgel pastes (125, 126), and clay suspensions (127, 128). The onset of such slip has been characterized by sliding yield stress (119, 126). The slip at the wall is profoundly influenced by the interaction between the material and the wall, whether attractive or repulsive (126, 129).

Shear Thickening

Shear thickening is a phenomenon in which the steady-state viscosity increases with increase in the shear rate. In a suspension of hard-spherical particles, shear thickening is experimentally

observed beyond the volume fraction of 0.3 (14). Typically at low shear rates, viscosity either remains constant or decreases with shear rate until a critical shear rate is reached, beyond which thickening is observed. The most commonly observed behavior is continuous shear thickening, wherein viscosity increases with a linear or weaker dependence on the shear rate. This behavior is hydrodynamic in origin and has been attributed to hydrocluster formation (130). In the vicinity of concentrations close to that associated with colloidal glass transition, discontinuous shear thickening (DST) is observed, wherein viscosity shows a very sharp rise with the increase in shear rate (131, 132), as shown in **Figure 3*i*** (133). It is believed that the origin of DST is not hydrodynamic but is in stress-induced jamming of the constituents. Holmes et al. (134) suggested that the caging phenomenon prevalent at high concentrations hinders translational mobility of particles. Consequently, the enhanced number of close contacts results in a dynamic arrest, causing the increase in τ_α and leading to DST. Recently, Seto et al. (135) reported that contact friction between the particles is necessary to observe DST. Prediction of discontinuous shear thickening was demonstrated by the soft glassy rheology (SGR) model (136) as well as mode-coupling theory (MCT) (137). Comprehensive discussions on shear thickening can be found in recent reviews (11, 131).

Compliance (J): in creep flow, compliance is strain induced in the material divided by constant stress

Creep flow: deformation of material under constant stress

MODELING APPROACHES

Model for Simple Yield-Stress Fluids

Simple yield-stress fluids, which are proposed to be invariant of time, follow a generic constitutive equation in tensorial form given by (65, 138)

$$\underset{\approx}{\sigma} = E\,\underset{\approx}{\gamma}, \quad \text{for } \sqrt{\underset{\approx}{\sigma} : \underset{\approx}{\sigma}/2} < \sigma_y$$

$$\underset{\approx}{\sigma} = \left(\frac{\sigma_y}{\dot{\gamma}} + \mu\right)\underset{\approx}{\dot{\gamma}}, \quad \text{for } \sqrt{\underset{\approx}{\sigma} : \underset{\approx}{\sigma}/2} \geq \sigma_y, \qquad 1.$$

where $\underset{\approx}{\sigma}$ is stress, $\underset{\approx}{\gamma}$ is strain, E is modulus, $\underset{\approx}{\dot{\gamma}}$ is rate of strain, σ_y is yield stress, and $\dot{\gamma} = \sqrt{\underset{\approx}{\dot{\gamma}} : \underset{\approx}{\dot{\gamma}}/2}$. A constant value of μ leads to the Bingham model, and $\mu = m\dot{\gamma}^{n-1}$, where m and n are constants, is the Herschel-Bulkley model. Subsequent to yielding, the Bingham plastic model shows a weak decrease in viscosity with shear rate compared with the Herschel-Bulkley model. A broad range of simple yield-stress fluids show good agreement with the Herschel-Bulkley model, and an example of a fit of Equation 1 to experimental data is shown in **Figure 3*e*** for a Carbopol gel (86).

Linear Viscoelasticity for Aging Soft Glassy Materials

All materials that follow time-translational invariance (TTI) obey the Boltzmann superposition principle (BSP). In the linear regime in the conventional BSP, response depends only on the time elapsed since application of an impetus. However, in glassy materials, owing to aging effects, response shows additional dependence on the time at which an impetus was applied (t_w). A modified expression of BSP for strain induced (γ, response) owing to imposed stress (σ, impetus) is given by (5)

$$\gamma(t) = \int_{-\infty}^{t} J(t - t_w, t_w)\frac{d\sigma}{dt_w}dt_w, \qquad 2.$$

where t is time and J is compliance.

The intricacies originating from additional time dependence can be eliminated by transforming the BSP from the real time (t) domain to the effective time (ξ) domain where the material becomes time invariant. For a material demonstrating $\tau = \tau(t)$, ξ is defined as (48) $\xi(t) = \int_0^t \tau_0 dt'/\tau(t')$,

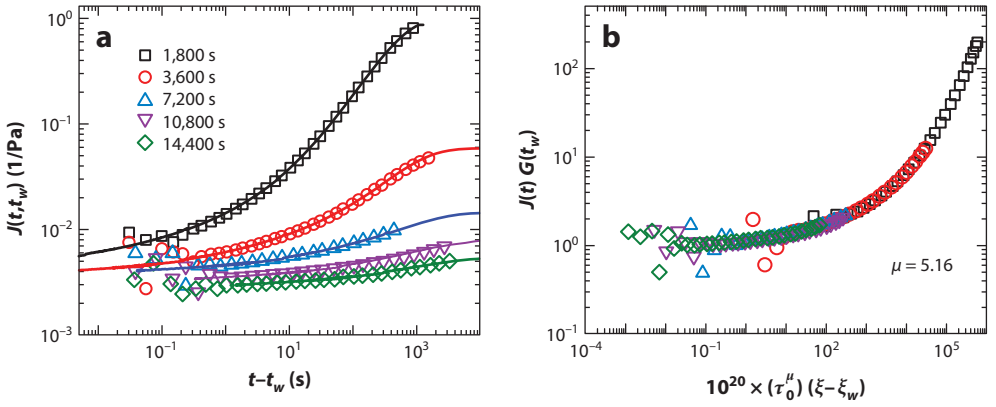

Figure 4

Evolution of compliance (*symbols*) is plotted as a function of creep time for different t_w in *a*. The transformation of creep data into the ξ domain leads to superposition (shown in *b*). Transformation of superposition from the ξ domain to the t domain leads to prediction of long and short time behavior, shown by lines in *a*. Data from Reference 48.

where τ_0 is the constant relaxation time associated with the ξ domain. BSP takes the same form in ξ domain as Equation 2, given by (5, 6, 48)

$$\gamma[\xi(t)] = \int_{-\infty}^{\xi(t)} J(\xi - \xi_w)\frac{d\sigma}{d\xi_w}d\xi_w, \qquad 3.$$

where $\xi_w = \xi(t_w)$. Interestingly, in the ξ domain, creep compliance is a function only of $\xi - \xi_w$. However, to express ξ domain, prior knowledge of the dependence $\tau = \tau(t)$ is necessary, which for glassy materials is usually given by $\tau = A\tau_m^{1-\mu}t^{\mu}$ (6, 39, 48–50, 80). Applicability of BSP in the ξ domain was validated by Shahin & Joshi (48), who carried out creep experiments on Laponite suspensions at different t_w, as shown in **Figure 4*a***, wherein J indeed shows an additional dependence on t_w. Remarkably, as shown in **Figure 4*b***, the same creep curves demonstrate an excellent superposition when plotted as a function of $\xi - \xi_w$. Shahin & Joshi (48) argued that the existence of such a superposition suggests that compliance induced in the material shall trace the path of superposition in the ξ domain irrespective of t_w and $t - t_w$. Consequently, transforming the superposition from the ξ domain back to the t domain facilitates prediction of the long time-creep behavior of aged samples (high t_w) through data obtained for young samples (low t_w), as shown in **Figure 4*a***.

Gupta et al. (61) carried out creep and step-strain experiments at different temperatures and validated the time-temperature superposition principle in the ξ domain. Similarly, Baldewa & Joshi (54) also verified the time-stress superposition. Recently, Kaushal & Joshi (55) demonstrated the validity of convolution relation between creep compliance and relaxation modulus in ξ domain for a variety of SGMs. However, it is important to note that observation of the superpositions confirms the validity of Equation 3 if the shape of the relaxation time spectrum is not affected by either t_w, T, or σ (7, 61). Applicability of BSP and time-temperature superposition to SGMs is an important step in analyzing the rheological behavior. However, there is a need for the complete description of linear viscoelastic principles in ξ domain, including Kramers–Kronig relations and various expressions relating relaxation and retardation time distributions to the rheological response functions. The complete description of linear viscoelasticity will also facilitate advancement in developing nonlinear viscoelastic models.

Phenomenological Toy Models for Aging SGMs

Development of rigorous constitutive equations from a microstructural point of view, particularly to explain the complex time dependency associated with the material behavior, is not an easy task. However, many phenomenological theories, or toy models, have been developed to qualitatively explain the physical behaviors. Mewis & Wagner (11, 139) have presented a detailed review of the phenomenological theories. These theories constitute three aspects (11, 140): the constitutive equation that relates σ, γ, and their time derivatives; a relation between the rheological parameters and an empirical structure parameter (λ) that describes the material state; and finally, the rate of evolution of λ as a function of time and deformation field. Most of the constitutive equations have a general form of the Herschel-Bulkley model represented by Equation 1, although in some cases the Maxwell model has been employed to induce elasticity. The viscosity and σ_y are usually increasing functions of λ, if not constant. An extensive list of such relations used in the literature can be found elsewhere (11, 139).

Maxwell model: a mechanical model with a Hookean spring and Newtonian dashpot in series

The structure represented by λ evolves with time essentially because of thermal motion (aging) and is destroyed by the deformation field (rejuvenation). The corresponding kinetic equation has a very general form described by (3)

$$\frac{d\lambda}{dt} = \frac{1}{\tau} - C(\lambda)\dot{\gamma}, \qquad 4.$$

where the first term on the right represents the buildup of structure with timescale τ and the second term represents the breakdown. One of the most notable proposals is by Coussot and coworkers (102), who consider $C(\lambda) \propto \lambda$ in Equation 4 and viscosity to be an increasing function of λ with a stronger-than-linear dependence. With this simple choice of λ, they show that viscosity increases continuously with time when σ is below a critical value, and the material is rejuvenated above the same, leading to viscosity bifurcation. Furthermore, the model suggests that the critical stress increases with an increase in the initial value of λ at which stress is applied, suggesting that σ_y depends on time. This simple model also demonstrates delayed yielding and shear banding. The very fact that the model represents structure using a single timescale, τ, suggests that alteration of the spectrum of relaxation times need not be invoked to explain behaviors such as viscosity bifurcation, delayed yielding, and shear banding.

Soft Glassy Rheology Model

Sollich et al. (5, 97, 141) presented the SGR model, which at present is the most comprehensive constitutive equation that explains most of the generic features of the SGMs. The SGR model, which is based on Bouchaud's trap model (142), considers an ensemble of mesoscopic elements with different yield energies or barrier heights, E. Under the application of a deformation field, the elements deform, affinely inducing local strain γ in each element. The element is elastically strained until the yield strain γ_y ($e_{dy} = \frac{1}{2}k\gamma_y^2$) is reached. Subsequent to yielding, elements get trapped in a new, unstrained environment ($\gamma = 0$). The SGR model also considers yielding to be an activated process, so that the mean lifetime of an element before yielding is $\tau = \tau_0 \exp[(E - e_d)/x]$, where τ_0 is an inverse of attempt frequency (τ^{-1} suggests rate of yielding) and x is a characteristic energy available for the activation process and is of the order of the mean barrier height. The expression of τ suggests that an element climbs the wall of the energy well by $e_d = \frac{1}{2}k\gamma^2$ so that the barrier to escape the well reduces to $E - \frac{1}{2}k\gamma^2$. Elements of SGM subsequent to mechanical quench are assigned barrier heights from a prior distribution, $\rho(E)$. Their occupancy probability, $P(E, \gamma, t)$, is the probability of finding an element trapped in a well with depth E and having strain

γ at time t, whose evolution is given by (97)

$$\frac{\partial P}{\partial t} = -\dot{\gamma}\frac{\partial P}{\partial \gamma} - \frac{P}{\tau} + \Gamma(t)\rho(E)\delta(\gamma), \qquad 5.$$

where $\Gamma(t) = \int\int (P/\tau) dE\, d\gamma$. The first term on the right represents the strained state before yielding, the second term describes diffusion out of the trap, and the third term accounts for trapping into a new well after yielding; the unit impulse function, δ, suggests this state to be unstrained (3). The SGR model uses the same form of $\rho(E) = (1/\langle E\rangle)\exp(-E/\langle E\rangle)$, as suggested by Bouchaud (142), which indicates a glass transition $k_B T_g = \langle E\rangle$ and shows aging for $x = k_B T < \langle E\rangle$. Finally, the stress induced in the material is given by $\sigma = k\int\int \gamma P dE d\gamma$ (97). The most important contribution of the SGR model is that it gives a description of the relaxation-time spectrum associated with the material at a given time for a given deformation field. This model led to successful descriptions of important phenomena demonstrated by SGM, such as aging and rejuvenation (thixotropy), yielding, and overaging. Recently, Fielding et al. (143) extended the SGR model to include the evolution of x originating from fluidity in the vicinity of particles. The modification allowed predictions of behaviors such as viscosity bifurcation and shear banding. The SGR framework is also shown to predict shear thickening by considering x to be a decreasing function of stress or strain, such that the application of the deformation field brings the material closer to the glass transition, causing enhancement in the relaxation time (136).

Mode Coupling Theory Approaches

At high volume fractions, particles are trapped in cages formed by their neighbors. Consequently, cage diffusion gets exceedingly slower with increased concentration. MCT proposes that cages are formed by the neighboring particles, which themselves are arrested. Therefore, there exists a nonlinear feed-forward mechanism that prevents the relaxation of fluctuations in local density toward the equilibrium state, leading to the glass transition (137). For spherical particles with hard-sphere interactions, MCT predicts an ideal glass transition at the volume fraction of 0.525, which is quite close to the experimentally observed value of 0.58 (144). At this volume fraction, the relaxation time diverges via a power law: $\tau_\alpha \propto (\phi_c - \phi)^{-2.58}$ (14). MCT, though mathematically intricate, is known to describe the dynamics in great detail in the vicinity of (but below) the glass transition. In **Figure 3*c***, we have plotted a fit of MCT to the frequency dependence of G' and G'' for a concentrated hard-sphere suspension (77). It can be seen that MCT does a good job of fitting the experimental data. In a recent study, MCT was reported to fully describe the linear viscoelastic behavior of colloidal suspensions (145). MCT has also been applied to clusters of particles rather than to individual particles, thereby extending the concept to the weak gels (146). However, the present formulations of MCT do not predict physical aging (147). For further discussion of the predictability and limitations of MCT, refer to Reference 148 and references therein.

Through a series of papers, Cates and coworkers (134, 137, 147, 149) modified MCT to account for the effect of the deformation field. They observed that owing to the deformation field, fluctuations in the local density field experience stronger restoring forces. Consequently, the α relaxation time decreases, allowing fluctuations to decay. By this mechanism, colloidal glasses jammed into arrested states can be made ergodic by application of a deformation field (137). Unlike the SGR model, this mechanism also predicts the presence of finite yield stress for colloidal suspensions at and above the glass transition. To investigate the discontinuous shear thickening, Holmes et al. (134) modified the MCT approach to incorporate stress-induced glass transition, which causes the divergence of the α relaxation time when stress is applied. The model predicts a gradual transition from continuous to discontinuous shear thickening as the concentration of

particles is increased. Brader et al. (147) recently proposed a single-mode MCT by incorporating a tensorial structure. Under the application of a combination of components of stress tensor, it leads to a yield surface that closely matches von Mises's criterion for yielding.

CONCLUSION

In this review, we present an overview of the structure and the rheological behavior of colloidal soft materials with soft-solid or paste-like consistencies that undergo a solid-liquid transition upon application of a deformation field. Depending upon the nature of constituents and resulting microstructure, these materials can be distinguished as colloidal glasses or gels. However, because in many systems the microstructure is too complex to allow such distinctions, the inclusive term SGM is used. These materials are usually thermodynamically out of equilibrium. Depending on the thermal energy associated with their constituents, these materials may show time-dependent structural recovery, a process known as aging. On the other hand, in the process of rejuvenation, the deformation field destroys the structure built during aging. Depending upon the nature and strength of the deformation field, competition between aging and rejuvenation leads to a rich spectrum of fascinating behaviors, such as overaging, viscosity bifurcation, delayed yielding, delayed solidification, and shear banding. Furthermore, various in situ optical tools have facilitated the correlation of the structure with the dynamics in this class of materials.

Theoretical treatment of SGMs has been a challenging task owing to time and deformation field–dependent rheological constitutive relations. On one hand, phenomenological toy models help clarify the underlying physical mechanisms behind the observed behaviors. On the other hand, models such as SGR and MCT are far more descriptive and mathematically involved and lead to greater insight into mesoscopic or microstructural dynamics. The linear viscoelasticity and time-temperature superposition developed for aging glassy materials essentially provide useful tools to analyze the experimental data. However, there is a great need for mathematical formulations that are simple enough to be used in simulation packages and that capture the basic quantitative description of the rheological behavior of SGMs. Such models can be used to simulate the realistic flow fields and can be applied to industrial materials to have efficient processing.

DISCLOSURE STATEMENT

The author is not aware of any affiliations, memberships, funding, or financial holdings that might be perceived as affecting the objectivity of this review.

ACKNOWLEDGMENTS

I acknowledge financial support from the Department of Atomic Energy–Science Research Council (DAE-SRC), Government of India. I also thank Anantha Ramakrishna, Ranjini Bandyopadhyay, and Raj Chhabra for their comments.

LITERATURE CITED

1. Israelachvili JN. 2010. *Intermolecular and Surface Forces*. London: Academic
2. Hunter GL, Weeks ER. 2012. The physics of the colloidal glass transition. *Rep. Prog. Phys.* 75:066501
3. Coussot P. 2007. Rheophysics of pastes: a review of microscopic modelling approaches. *Soft Matter* 3:528–40
4. Bandyopadhyay R, Liang D, Harden JL, Leheny RL. 2006. Slow dynamics, aging, and glassy rheology in soft and living matter. *Solid State Commun.* 139:589–98

5. Fielding SM, Sollich P, Cates ME. 2000. Aging and rheology in soft materials. *J. Rheol.* 44:323–69
6. Struik LCE. 1978. *Physical Aging in Amorphous Polymers and Other Materials*. Houston: Elsevier
7. McKenna GB, Narita T, Lequeux F. 2009. Soft colloidal matter: a phenomenological comparison of the aging and mechanical responses with those of molecular glasses. *J. Rheol.* 53:489–516
8. Di X, Win KZ, McKenna GB, Narita T, Lequeux F, et al. 2011. Signatures of structural recovery in colloidal glasses. *Phys. Rev. Lett.* 106:095701
9. Saha D, Joshi YM, Bandyopadhyay R. 2014. Investigation of the dynamical slowing down process in soft glassy colloidal suspensions: comparisons with supercooled liquids. *Soft Matter*. In press. doi:10.1039/C4SM00187G
10. Coussot P. 2005. *Rheometry of Pastes, Suspensions and Granular Materials: Application in Industry and Environment*. Hoboken: Wiley
11. Mewis J, Wagner NJ. 2012. *Colloidal Suspension Rheology*. Cambridge: Cambridge Univ. Press
12. Faraday Discuss. 2003. General discussion. *Faraday Discuss.* 123:75–97
13. Jones RAL. 2002. *Soft Condensed Matter*. Oxford: Oxford Univ. Press
14. Larson RG. 1999. *The Structure and Rheology of Complex Fluids*. Oxford: Clarendon Press
15. Pusey PN, van Megen W. 1987. Observation of a glass transition in suspensions of spherical colloidal particles. *Phys. Rev. Lett.* 59:2083–86
16. Russel WB, Saville DA, Schowalter WR. 1989. *Colloidal Dispersions*. Cambridge: Cambridge Univ. Press
17. Agarwal P, Qi H, Archer LA. 2009. The ages in a self-suspended nanoparticle liquid. *Nano Lett.* 10:111–15
18. Vlassopoulos D, Fytas G. 2010. From polymers to colloids: engineering the dynamic properties of hairy particles. *Adv. Polym. Sci.* 236:1–54
19. Solomon MJ, Spicer PT. 2010. Microstructural regimes of colloidal rod suspensions, gels, and glasses. *Soft Matter* 6:1391–400
20. Prasher R, Phelan PE, Bhattacharya P. 2006. Effect of aggregation kinetics on the thermal conductivity of nanoscale colloidal solutions (nanofluid). *Nano Lett.* 6:1529–34
21. Poon WCK, Haw MD. 1997. Mesoscopic structure formation in colloidal aggregation and gelation. *Adv. Colloid Interface Sci.* 73:71–126
22. Lu PJ, Weitz DA. 2013. Colloidal particles: crystals, glasses, and gels. *Annu. Rev. Condens. Matter Phys.* 4:217–33
23. Zaccarelli E, Poon WCK. 2009. Colloidal glasses and gels: the interplay of bonding and caging. *Proc. Natl. Acad. Sci. USA* 106:15203–8
24. Tanaka H, Meunier J, Bonn D. 2004. Nonergodic states of charged colloidal suspensions: repulsive and attractive glasses and gels. *Phys. Rev. E* 69:031404
25. Liu AJ, Nagel SR. 1998. Jamming is not just cool any more. *Nature* 396:21–22
26. Trappe V, Prasad V, Cipelletti L, Segre PN, Weitz DA. 2001. Jamming phase diagram for attractive particles. *Nature* 411:772–75
27. Meeker SP, Bonnecaze RT, Cloitre M. 2004. Slip and flow in pastes of soft particles: direct observation and rheology. *J. Rheol.* 48:1295–320
28. Höhler R, Cohen-Addad S. 2005. Rheology of liquid foam. *J. Phys. Condens. Matter* 17:R1041
29. Mason TG, Lacasse M-D, Grest GS, Levine D, Bibette J, Weitz DA. 1997. Osmotic pressure and viscoelastic shear moduli of concentrated emulsions. *Phys. Rev. E* 56:3150–66
30. Joshi YM. 2007. Model for cage formation in colloidal suspension of laponite. *J. Chem. Phys.* 127:081102
31. Ruzicka B, Zaccarelli E. 2011. A fresh look at Laponite phase diagram. *Soft Matter* 7:1268–86
32. Shahin A, Joshi YM. 2012. Physicochemical effects in aging aqueous Laponite suspensions. *Langmuir* 28:15674–86
33. Shalkevich A, Stradner A, Bhat SK, Muller F, Schurtenberger P. 2007. Cluster, glass, and gel formation and viscoelastic phase separation in aqueous clay suspensions. *Langmuir* 23:3570–80
34. Utracki LA. 2004. *Clay-Containing Polymeric Nanocomposites Volume 1*. Shawbury, UK: Rapra Technol.
35. Ren J, Casanueva BF, Mitchell CA, Krishnamoorti R. 2003. Disorientation kinetics of aligned polymer layered silicate nanocomposites. *Macromolecules* 36:4188–94
36. Shah SN, Ogugbue CC. 2010. *Future challenges of drilling fluids and their rheological measurements*. Presented at Am. Assoc. Drill. Eng. (AADE) Conf. Exhib., Houston TX

37. Brummer R. 2006. *Rheology Essentials of Cosmetic and Food Emulsions*. Berlin: Springer
38. McKeown SA, Mackley MR, Moggridge GD. 2003. Shear-induced structural changes in a commercial surfactant-based system. *Chem. Eng. Res. Des.* 81:649–64
39. Baldewa B, Joshi YM. 2011. Thixotropy and physical aging in acrylic emulsion paint. *Polym. Eng. Sci.* 51:2084–91
40. Food Agric. Organ./World Health Organ. 2010. *Manual on Development and Use of FAO and WHO Specifications for Pesticides*. Rome: World Health Organ./Food Agric. Organ.
41. Jarny S, Roussel N, Rodts S, Bertrand F, Le Roy R, Coussot P. 2005. Rheological behavior of cement pastes from MRI velocimetry. *Cem. Concr. Res.* 35:1873–81
42. Boger DV. 2013. Rheology of slurries and environmental impacts in the mining industry. *Annu. Rev. Chem. Biomol. Eng.* 4:239–57
43. Cipelletti L, Ramos L. 2005. Slow dynamics in glassy soft matter. *J. Phys. Cond. Mat.* 17:R253–R85
44. Viasnoff V, Jurine S, Lequeux F. 2003. How are colloidal suspensions that age rejuvenated by strain application? *Faraday Discuss.* 123:253–66
45. Viasnoff V, Lequeux F. 2002. Rejuvenation and overaging in a colloidal glass under shear. *Phys. Rev. Lett.* 89:065701
46. Shahin A, Joshi YM. 2012. Hyper-aging dynamics of nanoclay suspension. *Langmuir* 28:5826–33
47. Bandyopadhyay R, Liang D, Yardimci H, Sessoms DA, Borthwick MA, et al. 2004. Evolution of particle-scale dynamics in an aging clay suspension. *Phys. Rev. Lett.* 93:228302
48. Shahin A, Joshi YM. 2011. Prediction of long and short time rheological behavior in soft glassy materials. *Phys. Rev. Lett.* 106:038302
49. Derec C, Ducouret G, Ajdari A, Lequeux F. 2003. Aging and nonlinear rheology in suspensions of polyethylene oxide-protected silica particles. *Phys. Rev. E* 67:061403
50. Negi AS, Osuji CO. 2009. Dynamics of internal stresses and scaling of strain recovery in an aging colloidal gel. *Phys. Rev. E* 80:010404
51. Bissig H, Romer S, Cipelletti L, Trappe V, Schurtenberger P. 2003. Intermittent dynamics and hyper-aging in dense colloidal gels. *Phys. Chem. Comm.* 6:21–23
52. Coussot P, Tabuteau H, Chateau X, Tocquer L, Ovarlez G. 2006. Aging and solid or liquid behavior in pastes. *J. Rheol.* 50:975–94
53. Awasthi V, Joshi YM. 2009. Effect of temperature on aging and time-temperature superposition in nonergodic Laponite suspensions. *Soft Matter* 5:4991–96
54. Baldewa B, Joshi YM. 2012. Delayed yielding in creep, time-stress superposition and effective time theory for a soft glass. *Soft Matter* 8:789–96
55. Kaushal M, Joshi YM. 2014. Linear viscoelasticity of soft glassy materials. *Soft Matter* 12:1891–94
56. Zargar R, Nienhuis B, Schall P, Bonn D. 2013. Direct measurement of the free energy of aging hard sphere colloidal glasses. *Phys. Rev. Lett.* 110:258301
57. Stiakakis E, Wilk A, Kohlbrecher J, Vlassopoulos D, Petekidis G. 2010. Slow dynamics, aging, and crystallization of multiarm star glasses. *Phys. Rev. E* 81:020402
58. Manley S, Davidovitch B, Davies NR, Cipelletti L, Bailey AE, et al. 2005. Time-dependent strength of colloidal gels. *Phys. Rev. Lett.* 95:048302
59. Malkin AY, Isayev AI. 2006. *Rheology: Concepts, Methods, and Applications*. Toronto: Chemtec Publ.
60. Ovarlez G, Coussot P. 2007. Physical age of soft-jammed systems. *Phys. Rev. E* 76:011406
61. Gupta R, Baldewa B, Joshi YM. 2012. Time temperature superposition in soft glassy materials. *Soft Matter* 8:4171–76
62. Dhavale TP, Jatav S, Joshi YM. 2013. Thermally activated asymmetric structural recovery in a soft glassy nano-clay suspension. *Soft Matter* 9:7751–56
63. Agarwal P, Srivastava S, Archer LA. 2011. Thermal jamming of a colloidal glass. *Phys. Rev. Lett.* 107:268302
64. Ovarlez G, Barral Q, Coussot P. 2010. Three-dimensional jamming and flows of soft glassy materials. *Nat. Mater.* 9:115–19
65. Shaukat A, Kaushal M, Sharma A, Joshi YM. 2012. Shear mediated elongational flow and yielding in soft glassy materials. *Soft Matter* 8:10107–14

66. Negi A, Osuji C. 2010. Dynamics of a colloidal glass during stress-mediated structural arrest. *Europhys. Lett.* 90:28003
67. Manneville S. 2008. Recent experimental probes of shear banding. *Rheol. Acta* 47:301–18
68. Isa L, Besseling R, Schofield AB, Poon WCK. 2010. Quantitative imaging of concentrated suspensions under flow. *Adv. Polym. Sci.* 236:163–202
69. Pignon F, Magnin A, Piau J-M. 1997. Butterfly light scattering pattern and rheology of a sheared thixotropic clay gel. *Phys. Rev. Lett.* 79:4689–92
70. Philippe AM, Baravian C, Imperor-Clerc M, Silva JD, Paineau E, et al. 2011. Rheo-SAXS investigation of shear-thinning behaviour of very anisometric repulsive disc-like clay suspensions. *J. Phys. Condens. Matter* 23:194112
71. Stellbrink J, Lonetti B, Rother G, Willner L, Richter D. 2008. Shear induced structures of soft colloids: Rheo-SANS experiments on kinetically frozen PEP–PEO diblock copolymer micelles. *J. Phys. Condens. Matter* 20:404206
72. Cicuta P, Donald AM. 2007. Microrheology: a review of the method and applications. *Soft Matter* 3:1449–55
73. Squires TM, Mason TG. 2010. Fluid mechanics of microrheology. *Annu. Rev. Fluid Mech.* 42:413–38
74. Oppong FK, Coussot P, de Bruyn JR. 2008. Gelation on the microscopic scale. *Phys. Rev. E* 78:021405
75. Rich JP, McKinley GH, Doyle PS. 2011. Size dependence of microprobe dynamics during gelation of a discotic colloidal clay. *J. Rheol.* 55:273–99
76. Trappe V, Weitz DA. 2000. Scaling of the viscoelasticity of weakly attractive particles. *Phys. Rev. Lett.* 85:449–52
77. Mason TG, Weitz DA. 1995. Linear viscoelasticity of colloidal hard sphere suspensions near the glass transition. *Phys. Rev. Lett.* 75:2770–73
78. Winter HH. 2013. Glass transition as the rheological inverse of gelation. *Macromolecules* 46:2425–32
79. Ikeda A, Berthier L, Sollich P. 2013. Disentangling glass and jamming physics in the rheology of soft materials. *Soft Matter* 9:7669–83
80. Cloitre M, Borrega R, Leibler L. 2000. Rheological aging and rejuvenation in microgel pastes. *Phys. Rev. Lett.* 85:4819–22
81. Joshi YM, Reddy GRK. 2008. Aging in a colloidal glass in creep flow: time-stress superposition. *Phys. Rev. E* 77:021501
82. Joshi YM, Reddy GRK, Kulkarni AL, Kumar N, Chhabra RP. 2008. Rheological behavior of aqueous suspensions of laponite: new insights into the ageing phenomena. *Proc. R. Soc. A* 464:469–89
83. Barnes HA. 1997. Thixotropy—a review. *J. Non-Newton. Fluid Mech.* 70:1–33
84. Negi AS, Osuji CO. 2010. Time-resolved viscoelastic properties during structural arrest and aging of a colloidal glass. *Phys. Rev. E* 82:031404
85. Moller P, Fall A, Chikkadi V, Derks D, Bonn D. 2009. An attempt to categorize yield stress fluid behaviour. *Philos. Trans. R. Soc. A Math. Phys. Eng. Sci.* 367:5139–55
86. Boujlel J, Coussot P. 2013. Measuring the surface tension of yield stress fluids. *Soft Matter* 9:5898–908
87. Kamble S, Pandey A, Rastogi S, Lele A. 2013. Ascertaining universal features of yielding of soft materials. *Rheol. Acta* 52:859–65
88. Barnes HA. 1999. The yield stress—a review or '$\pi\alpha\nu\tau\alpha\ \rho\varepsilon\iota$'—everything flows? *J. Non-Newton. Fluid Mech.* 81:133–78
89. Hill R. 1950. *The Mathematical Theory of Plasticity*. New York: Oxford Univ. Press
90. Koumakis N, Petekidis G. 2011. Two step yielding in attractive colloids: transition from gels to attractive glasses. *Soft Matter* 7:2456–70
91. Shao Z, Negi AS, Osuji CO. 2013. Role of interparticle attraction in the yielding response of microgel suspensions. *Soft Matter* 9:5492–500
92. Pham KN, Petekidis G, Vlassopoulos D, Egelhaaf SU, Pusey PN, Poon WCK. 2006. Yielding of colloidal glasses. *Europhys. Lett.* 75:624–30
93. Kramb RC, Zukoski CF. 2011. Yielding in dense suspensions: cage, bond, and rotational confinements. *J. Phys. Condens. Matter* 23:035102
94. Sentjabrskaja T, Babaliari E, Hendricks J, Laurati M, Petekidis G, Egelhaaf SU. 2013. Yielding of binary colloidal glasses. *Soft Matter* 9:4524–33

95. Kramb RC, Zukoski CF. 2011. Nonlinear rheology and yielding in dense suspensions of hard anisotropic colloids. *J. Rheol.* 55:1069–84
96. Eyring H. 1936. Viscosity, plasticity, and diffusion as examples of absolute reaction rates. *J. Chem. Phys.* 4:283–91
97. Sollich P, Lequeux F, Hebraud P, Cates ME. 1997. Rheology of soft glassy materials. *Phys. Rev. Lett.* 78:2020–23
98. Petekidis G, Vlassopoulos D, Pusey PN. 2004. Yielding and flow of sheared colloidal glasses. *J. Phys. Condens. Matter* 16:S3955–63
99. Bandyopadhyay R, Mohan H, Joshi YM. 2010. Stress relaxation in aging soft colloidal glasses. *Soft Matter* 6:1462–68
100. Wallace ML, Joós B. 2006. Shear-induced overaging in a polymer glass. *Phys. Rev. Lett.* 96:025501
101. Kaushal M, Joshi YM. 2013. Tailoring relaxation time spectrum in soft glassy materials. *J. Chem. Phys.* 139:024904
102. Coussot P, Nguyen QD, Huynh HT, Bonn D. 2002. Viscosity bifurcation in thixotropic, yielding fluids. *J. Rheol.* 46:573–89
103. Sprakel J, Lindström SB, Kodger TE, Weitz DA. 2011. Stress enhancement in the delayed yielding of colloidal gels. *Phys. Rev. Lett.* 106:248303
104. Gopalakrishnan V, Zukoski CF. 2007. Delayed flow in thermo-reversible colloidal gels. *J. Rheol.* 51:623–44
105. Shukla A, Joshi YM. 2009. Ageing under oscillatory stress: role of energy barrier distribution in soft glassy materials. *Chem. Eng. Sci.* 64:4668–74
106. Joshi YM, Shahin A, Cates ME. 2012. Delayed solidification of soft glasses: new experiments, and a theoretical challenge. *Faraday Discuss.* 158:313–24
107. Bird RB, Armstrong RC, Hassager O. 1987. *Dynamics of Polymeric Liquids, Volume 1. Fluid Mechanics.* New York: Wiley-Intersci.
108. Ovarlez G, Rodts S, Chateau X, Coussot P. 2009. Phenomenology and physical origin of shear localization and shear banding in complex fluids. *Rheol. Acta* 48:831–44
109. Paredes J, Shahidzadeh-Bonn N, Bonn D. 2011. Shear banding in thixotropic and normal emulsions. *J. Phys. Condens. Matter* 23:284116
110. Gibaud T, Frelat D, Manneville S. 2010. Heterogeneous yielding dynamics in a colloidal gel. *Soft Matter* 6:3482–88
111. Moorcroft RL, Cates ME, Fielding SM. 2011. Age-dependent transient shear banding in soft glasses. *Phys. Rev. Lett.* 106:055502
112. Divoux T, Tamarii D, Barentin C, Manneville S. 2010. Transient shear banding in a simple yield stress fluid. *Phys. Rev. Lett.* 104:208301
113. Martin JD, Hu YT. 2012. Transient and steady-state shear banding in aging soft glassy materials. *Soft Matter* 8:6940–49
114. Gibaud T, Barentin C, Taberlet N, Manneville S. 2009. Shear-induced fragmentation of Laponite suspensions. *Soft Matter* 5:3026–37
115. Rodts S, Baudez JC, Coussot P. 2005. From "discrete" to "continuum" flow in foams. *Europhys. Lett.* 69:636
116. Vasu KS, Krishnaswamy R, Sampath S, Sood AK. 2013. Yield stress, thixotropy and shear banding in a dilute aqueous suspension of few layer graphene oxide platelets. *Soft Matter* 9:5874–82
117. Besseling R, Isa L, Ballesta P, Petekidis G, Cates ME, Poon WCK. 2010. Shear banding and flow-concentration coupling in colloidal glasses. *Phys. Rev. Lett.* 105:268301
118. Aral BK, Kalyon DM. 1994. Effects of temperature and surface roughness on time-dependent development of wall slip in steady torsional flow of concentrated suspensions. *J. Rheol.* 38:957–72
119. Ballesta P, Petekidis G, Isa L, Poon WCK, Besseling R. 2012. Wall slip and flow of concentrated hard-sphere colloidal suspensions. *J. Rheol.* 56:1005–37
120. Ballesta P, Koumakis N, Besseling R, Poon WCK, Petekidis G. 2013. Slip of gels in colloid-polymer mixtures under shear. *Soft Matter* 9:3237–45
121. Persello J, Magnin A, Chang J, Piau JM, Cabane B. 1994. Flow of colloidal aqueous silica dispersions. *J. Rheol.* 38:1845–69

122. Egger H, McGrath KM. 2006. Estimating depletion layer thickness in colloidal systems: correlation with oil-in-water emulsion composition. *Colloids Surf. A Physicochem. Eng. Asp.* 275:107–13
123. Plucinski J, Gupta RK, Chakrabarti S. 1998. Wall slip of mayonnaises in viscometers. *Rheol. Acta* 37:256–69
124. Denkov ND, Subramanian V, Gurovich D, Lips A. 2005. Wall slip and viscous dissipation in sheared foams: effect of surface mobility. *Colloids Surf. A Physicochem. Eng. Aspects* 263:129–45
125. Bertola V, Bertrand F, Tabuteau H, Bonn D, Coussot P. 2003. Wall slip and yielding in pasty materials. *J. Rheol.* 47:1211–26
126. Seth JR, Cloitre M, Bonnecaze RT. 2008. Influence of short-range forces on wall-slip in microgel pastes. *J. Rheol.* 52:1241–68
127. Pignon F, Magnin A, Piau JM. 1996. Thixotropic colloidal suspensions and flow curves with minimum: identification of flow regimes and rheometric consequences. *J. Rheol.* 40:573–87
128. Shaukat A, Sharma A, Joshi YM. 2012. Squeeze flow behavior of (soft glassy) thixotropic material. *J. Non-Newton. Fluid Mech.* 167–68:9–17
129. Seth JR, Locatelli-Champagne C, Monti F, Bonnecaze RT, Cloitre M. 2012. How do soft particle glasses yield and flow near solid surfaces? *Soft Matter* 8:140–48
130. Wagner NJ, Brady JF. 2009. Shear thickening in colloidal dispersions. *Phys. Today* 62:27–32
131. Brown E, Jaeger HM. 2014. Shear thickening in concentrated suspensions: phenomenology, mechanisms, and relations to jamming. *Soft Condens. Matter.* In press. arXiv:1307.0269
132. Fagan ME, Zukoski CF. 1997. The rheology of charge stabilized silica suspensions. *J. Rheol.* 41:373–97
133. Hoffman RL. 1972. Discontinuous and dilatant viscosity behavior in concentrated suspensions. I. Observation of a flow instability. *Trans. Soc. Rheol.* 16:155–73
134. Holmes CB, Cates ME, Fuchs M, Sollich P. 2005. Glass transitions and shear thickening suspension rheology. *J. Rheol.* 49:237–69
135. Seto R, Mari R, Morris JF, Denn MM. 2013. Discontinuous shear thickening of frictional hard-sphere suspensions. *Phys. Rev. Lett.* 111:218301
136. Head DA, Ajdari A, Cates ME. 2001. Jamming, hysteresis, and oscillation in scalar models for shear thickening. *Phys. Rev. E* 64:061509
137. Cates ME. 2006. Yielding and jamming of dense suspensions. In *Jamming, Yielding, and Irreversible Deformation in Condensed Matter*, ed. MC Miguel, M Rubi, pp. 3–21. Berlin: Springer-Verlag
138. Denn MM. 1998. Are plug-flow regions possible in fluids exhibiting a yield stress? In *Dynamics of Complex Fluids*, ed. MJ Adams, RA Mashelkar, JRA Pearson, AR Rennie, pp. 372–78. London: Imp. Coll. Press
139. Mewis J, Wagner NJ. 2009. Thixotropy. *Adv. Colloid Interface Sci.* 147–48:214–27
140. Beris AN, Stiakakis E, Vlassopoulos D. 2008. A thermodynamically consistent model for the thixotropic behavior of concentrated star polymer suspensions. *J. Non-Newton. Fluid Mech.* 152:76–85
141. Sollich P. 1998. Rheological constitutive equation for a model of soft glassy materials. *Phys. Rev. E* 58:738–59
142. Bouchaud JP. 1992. Weak ergodicity breaking and aging in disordered systems. *J. Phys. I* 2:1705–13
143. Fielding SM, Cates ME, Sollich P. 2009. Shear banding, aging and noise dynamics in soft glassy materials. *Soft Matter* 5:2378–82
144. Gotze W, Sjogren L. 1992. Relaxation processes in supercooled liquids. *Rep. Prog. Phys.* 55:241
145. Siebenbürger M, Fuchs M, Winter H, Ballauff M. 2009. Viscoelasticity and shear flow of concentrated, noncrystallizing colloidal suspensions: comparison with mode-coupling theory. *J. Rheol.* 53:707–26
146. Kroy K, Cates ME, Poon WCK. 2004. Cluster mode-coupling approach to weak gelation in attractive colloids. *Phys. Rev. Lett.* 92:148302
147. Brader JM, Voigtmann T, Fuchs M, Larson RG, Cates ME. 2009. Glass rheology: from mode-coupling theory to a dynamical yield criterion. *Proc. Natl. Acad. Sci. USA* 106:15186–91
148. Schweizer KS. 2007. Dynamical fluctuation effects in glassy colloidal suspensions. *Curr. Opin. Colloid Interface Sci.* 12:297–306
149. Fuchs M, Cates ME. 2009. A mode coupling theory for Brownian particles in homogeneous steady shear flow. *J. Rheol.* 53:957–1000